Green Light Luminescence from ZnO/Dodecylamine Mesolamellar Nanocomposites Synthesized by Self-Assembly

Yu-de Wang,*[a] Shuo Zhang,[a] and Xing-hui Wu[a]

Keywords: Mesoporous materials / Nanocomposites / Luminescence / Interfacial interactions

The synthesis, structural characterization and optical properties of a semiconducting zinc oxide based dodecylamine surfactant, mesolamellar zinc oxide/surfactant nanocomposite (Zn-L) are described. XRD and TEM results showed the formation of a lamellar mesostructure with two layer spacings ca. 28 Å. A red-shift in the absorption band edge of absorption spectrum and the green light photoluminescence of the resulted nanocomposite were observed at room temperature. The red-shift of the absorption band edge and the room temperature photoluminescence (RTPL) of the Zn-L nanocomposite might be induced by the dielectric confinement effect and the interfacial interaction between the ZnO and the surfactant, respectively.

Introduction

Recent developments in the synthesis of self-assembled inorganic/organic surfactant composites have opened up a new field in the study of composite materials.[1] Lamellar inorganic species/surfactant composite consist of surfactant layers, alternating with inorganic layers. When the inorganic layers are semiconducting materials, a novel nanostructured semiconductor–surfactant superlattice may result with, possibly,novel properties.[2] A novel chemical synthetic approach based on self-assembly between inorganic species and surfactant has been presented for inorganic species and organic surfactant into two- and three-dimensional superlattice structures,[3,4] and has been successfully extended to numerous ordered inorganic–organic composites with nanometer scale periodicities.[2,5] To date, a series of semiconductor lamellar mesophase in which a semiconductor oxide is sandwiched between organic components has been successfully synthesized.[6–8] Zinc oxide is a promising luminescent material with a wide bandgap (3.37 eV), large exciton binding energy (60 meV) and is used for various applications such as vacuum fluorescent displays due to its nonlinear optical properties and room temperature ultraviolet emission.[9] As a large-bandgap semiconductor and luminescence material, nanostructured ZnO (nanoparticles, nanowires, nanobelts, and nanotuble) has been widely studied.[10–12] However, to the best of our knowledge, ZnO lamellar mesophase, relative to its room temperature photoluminescence, has rarely been mentioned. In this letter, we report the synthesis and room temperature photoluminescence of a mesolamellar zinc oxide/surfactant nanocomposite, the morphology of which appears to be distinctively different from those previously reported.

[a] Department of Materials Science & Engineering, Yunnan University,
Kunming 650091, China
Fax: (internat.) +86-871-515-3832
E-mail: wangyude@tsinghua.org.cn

Results and Discussion

Powder XRD data clearly demonstrate the ordered lamellar mesostructure of the zinc oxide/surfactant composite (Figure 1): a series of equally spaced peaks appear in the low-angle region. Similar to lamellar silicate, aluminophosphate, and TiO_2 mesophase,[1,2] the peaks are attributed to the 00*l* rational reflections, characteristic of a lamellar structure. The first diffraction peak, assumed to be (001), corresponds to a *d*-spacing of about 28.5 Å. Reflections up to the 5th order of the (001) diffraction are observed. Besides the (00*l*) series, other diffraction peaks in the low-angle diffraction region are best assigned to positional ordering of the dodecylamine molecules within the bilayer. The fully extended dodecylamine bilayer can be estimated to be about 39 Å long. Crystalline dodecylamine displays a very similar XRD patter in this range.

The powder XRD pattern of the Zn-L composite clearly displays the characteristics of a well-ordered layered structure with evidence of registry between the sheets. The flaky morphology of Zn-L the composite, displayed in the SEM image, Figure 2(a), supports this proposal. The lamellar composite is further confirmed by a TEM study. Well-defined parallel lines [Figure 2(b)] confirm that the Zn-L composite is a lamellar structure[3] – consistent with the results of XRD. The inter-lamellar distance is 28 Å, in accordance with the *d*-spacing calculated from the first diffraction peak in the XRD pattern.

The FT-IR spectrum of the Zn-L composite shows a zinc–oxygen stretching band in the region 500–1000 cm^{-1}

 DOI: 10.1002/ejic.200400450

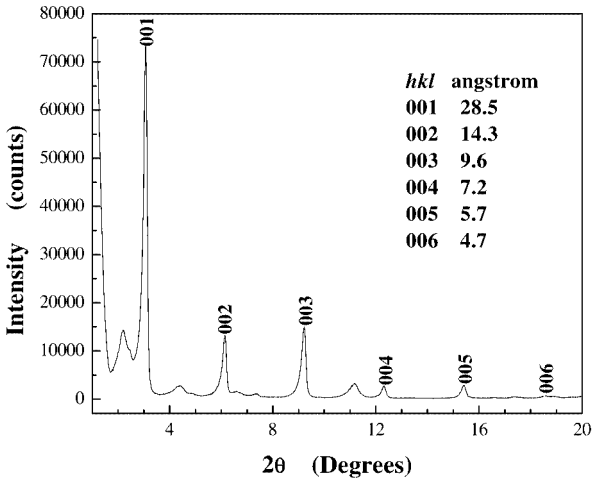

Figure 1. XRD pattern of as-synthesized Zn-L composite.

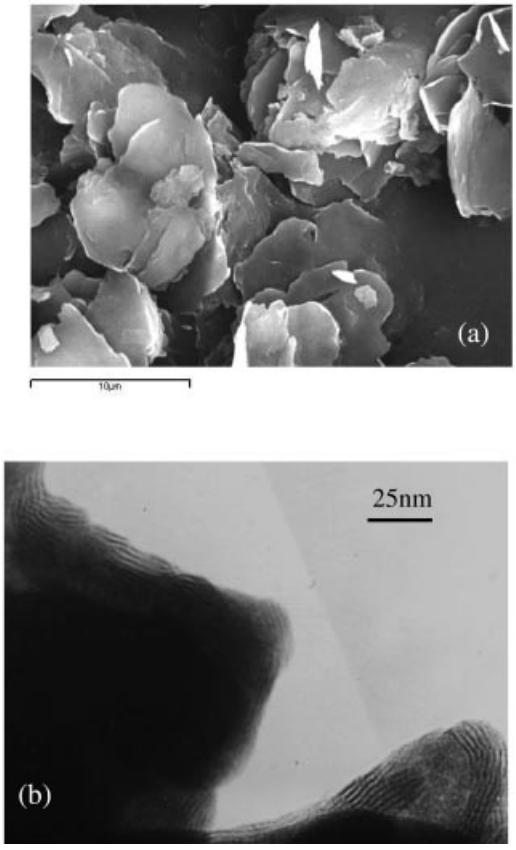

Figure 2. (a) Representative SEM image of Zn-L composite. (b) TEM image to the Zn-L composite showing the lamellar.

(Figure 3). Some bands in the region 3300–3500 cm^{-1} are due to N–H stretches of DDA, and sharp bands at 2853 and 2913 cm^{-1} are due to C–H stretches of the hydrocarbon chain of DDA. Sharp bands in the region 1370–1600 cm^{-1} are attributed to the deformation of $–CH_2–$ and $–CH_3$ of the incorporated DDA. The CH_2 stretching vibrations are considered to be related with the physical state (monomer, micelle or solid) of dodecylamine. These band vibrations indicate that the dodecylamine is present in the as-synthesized nickel oxide mesostructure. They provide evidence for the incorporation of dodecylamine into the hydrous oxide.[13] Figure 3 also reveals a C–N band at 1333 cm^{-1}, which is blue-shifted by 33 cm^{-1} compared with the spectrum of DDA (C–N at 1300 cm^{-1}). The affinity of Zn^{2+} ions to amine and imine ligands is well known. This allows us to assume chemical interaction between NHgroups of the DDA chains and surface Zn^{2+} ions of the Zn-L nanocomposites. It can be inferred that the formation of new surface states may results from chemical binding between the components of the neighbouring layers.

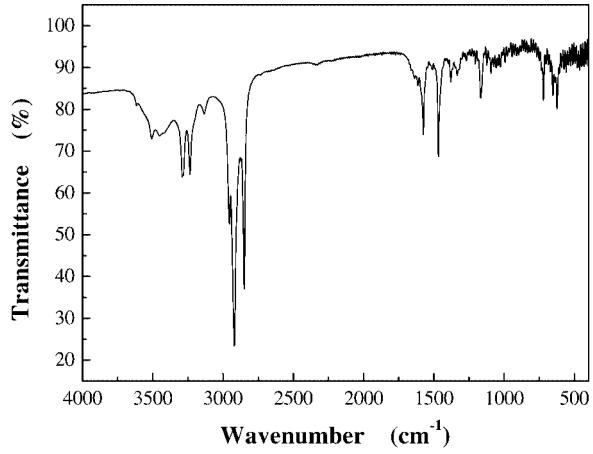

Figure 3. FTIR spectrum of Zn-L nanocomposite.

The two XPS spectrum peaks [Figure 4(a)], of $2p_{\frac{3}{2}}$ and $2p_{\frac{1}{2}}$ at 1022.9 eV and 1045.9 eV, with a better symmetry, are assigned to lattice zinc in zinc oxide. The peaks are 23.0 eV apart. The values correspond to a 2p3 binding energy of Zn^{II} ion (indexed Standard ESCA Spectra of the Elements and Line Energy Information, Φ Co., USA). The small shift in the $2p_{\frac{3}{2}}$ peak position from the crystalline ZnO to the mesolamellar structure ZnO, from 1021.7 eV (indexed Hand of X-ray photoelectron spectroscopy) to 1022.9 eV, indicates a change of microenvironments for zinc. This shift (1.2 eV) confirms that most Zn atoms remain in Zn-L nanocomposites, in the same formal valence state of Zn^{2+} within an oxygen deficient ZnO_{1-x} matrix.[14,15] This Zn enrichment or oxygen defects is due to the strong interaction between the dodecylamine and ZnO and to the weakly crystalline nature of the hydrous zinc oxide composite. Figure 4(b) shows that the O_{1s} XPS is asymmetric (the left-hand side is wider), indicating that there at least two kinds of oxygen species in the near surface region. The peak at about 531.6 eV is due to the ZnO crystal lattice oxygen, while that at about 533 eV is due to chemisorded oxygen.[16]

The lamellar mesostructured zinc oxide/surfactant composite displays interesting optical properties. UV/Vis spectroscopy was used to characterize the optical absorbance of the Zn-L nanocomposite. The absorption spectrum of Zn-L was carried out to resolve the excitonic or interband (valence-conduction band) transition of Zn-L, which allows us to calculate the bandgap. The absorption and corresponding bandgap energy of bulk ZnO is λ = 367 nm and E_g = 3.36 eV. The UV/Vis absorption spectrum of the as-synthe-

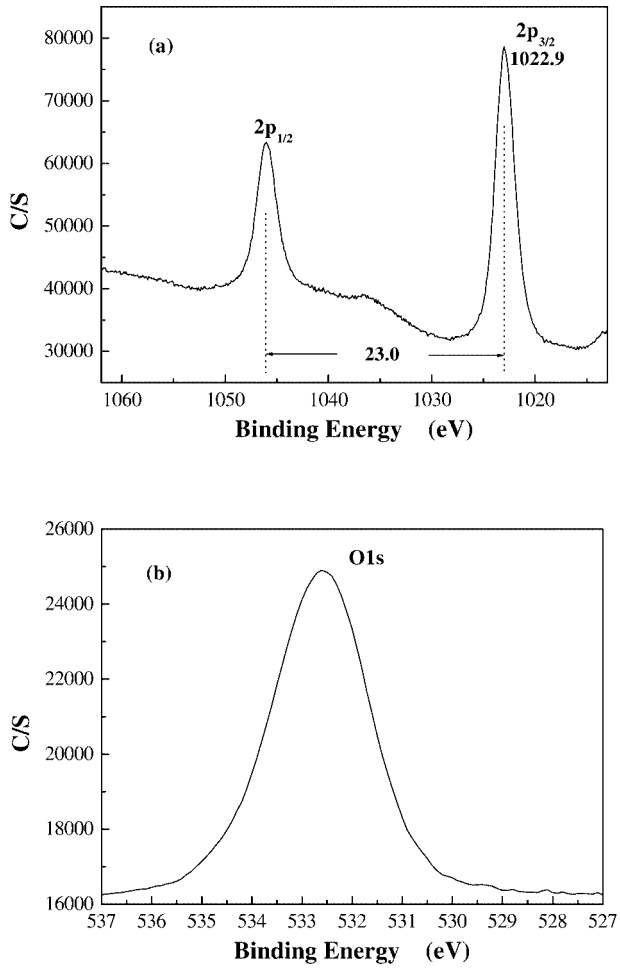

Figure 4. XPS spectra of ZnO/surfactant nanocomposites: (a) Zn2p and (b) O1s.

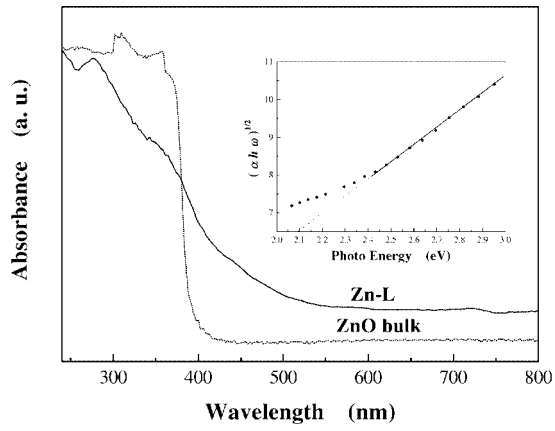

Figure 5. Absorption spectra of Zn-L composite and ZnO bulk. Inset: apparent energy gap of the Zn-L composite.

sized compositeshows a strong band edge absorption in the region above 370 nm (Figure 5). The absorption edge of Zn-L composite is red-shifted from the absorption edges of wurtzite ZnO dendrites (377 nm)[17] and bulk ZnO (367 nm). Absorption at longer wavelengths, the absorption red-shift, was also observed by Wang et al.[18] with sodium dodecylbenzenesulfonate (DBS) capped ZnO nanoparticles. The authors attributed this red-shift to intraband surface states formed by surfactant molecules chemically bound on the ZnO surface.

The absorption coefficient of an amorphous semiconductor has a characteristic relation:[19]

$$[d\hbar\omega]^{1/2} = A[\hbar\omega - E_g]$$

in which $\hbar\omega$ is the photon energy, E_g is the apparent optical bandgap, A is a constant characteristic of the amorphous semiconductor, and a is the absorption coefficient. Therefore, the E_g of zinc oxide/surfactant composite can be obtained by extrapolating the above relation to 2.09 eV (Figure 5 inset). A red-shift of ca. 1.27 eV relative to bulk ZnO is evident for the zinc oxide/surfactant inorganic–organic composite. This is contrary to the quantum size effect, which leads to a blue-shift of E_g with decreasing particle size, and has been observed in many nanometer-sized semiconductor materials.[20] Notably, however, the red-shift of absorption spectrum or apparant optical bandgap here would arise from the interface between zinc oxide and surfactant. As for the band edge shift of optical absorption of semiconductor nanoparticals in different surrounding mediums with a smaller dielectric constant than that of the semiconductors, Takagahara[21] attributes it to the dielectric confinement effect. He expressed, approximately,the bandgap of the semiconductor nanoparticles in the different surrounding mediums as

$$E_g = E_0 + \frac{\pi^2}{\bar{R}^2} - \frac{3.572}{\bar{R}} - \frac{0.248\varepsilon_1}{\varepsilon_2}$$

where E_0 is the bandgap of bulk semiconductor, $\bar{R} = R/a_B$ (R is semiconductor nanoparticles radius, a_B is exciton Bohr radius),and ε_1 and ε_2 are the dielectric constants of the semiconductor and surrounding medium, respectively. The second term is the quantum confinement energy, leading to the absorption band edge blue-shift as the size of particle radius reduces; the third term is the direct Coulomb interaction between an electron and a hole, leading to red-shift. The last term is usually called the surface polarization energy, which arises from the difference in dielectric constant between the semiconductor nanoparticles and the surrounding medium, leading to a red-shift. The dielectric confinement has a significant effect on the excition energy and can not be treated as a minor perturbation.[21] Therefore, the smallerthe semiconductor nanoparticles and the greater the difference between ε_1 and ε_2 , the greater the dielectric confinement effect becomes. For the Zn-L nanocomposites, the surfactant DDA has a smaller dielectric constant ($\varepsilon_1 \approx 1.5$) than ZnO ($\varepsilon_2 \approx 12$). The dielectric-constant ration $\varepsilon_2/\varepsilon_1$ is 8 and the dielectric confinement effect would be significant. When the dielectric confinement effect emerges, the screening effect is reduced and the Coulomb interaction between charged particles becomes enhanced, resulting in enhancement of the exciton binding energy and the exciton

oscillation strength; thus the surface polarization energy becomes the key factor influencing the absorption band edge.[21,22] Meanwhile, the quantum confinement energy would become the subordinate factor.

The room temperature emission spectrum of the Zn-L lamellar mesophase (Figure 6) shows that the RTPL of as-synthesized Zn-L exhibits a broad, strong emission band between 440 and 560 nm, centered at 480 nm (2.58 eV), i.e. in the green region of visible range. Compared with ZnO nanowires previously reported[23] and nanosheets,[17] the Zn-L lamellar mesophase shows a peak small shift about 20 nm and 6 nm, respectively. The maximum Stokes shift $\frac{1}{2}\Delta_{max}$ ($\hbar\omega_{ex} - \hbar\omega_{em}$) is 0.327 eV. Figure 6 shows that the board emission band is asymmetric (the right-hand side is wider), indicating that the emission band is made up of at least two overlapping emission bands, and the position of the overall maximum will depend on their intensity ratios. Inner interfacial defects between the ZnO and surfactant contribute to the relatively shorter wavelength of luminescence (<480 nm), while the outmost surfactant can additionally luminescence at long wavelengths (>480 nm).[18] Similar results and discussion have been reported by Lin[2] et al. for mesolamellar TiO_2. The luminescence of the Zn-L nanocomposite is similar to that from ZnO-capped sodium dodecylbenzenesulfonate.[18] The luminescence mechanisms of ZnO have been studied for several decades.[17,23] The ultraviolet peaks can be assigned to the direct recombination of a conduction electron and a hole in the valence band, and the green peaks can be attributed to the deep-trap-mediated emission. The origin of the deep trap in ZnO is not yet clearly understood but is generally attributed to structural defects, single ionized vacancies, and impurities.[23–26]

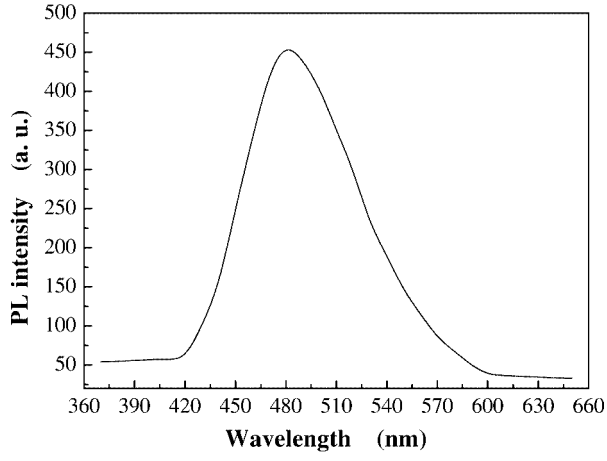

Figure 6. Emission (λ_{ex} = 383 nm) spectra of Zn-L nanocomposites.

In our investigation, the RTPL mechanism of Zn-L composite differs from that of bulk and other nanostructured ZnO. The mesolamellar zinc oxide/surfactant nanocomposites show the ordered structure to form zinc oxide/surfactant superlattices. This peculiar structure might have a profound effect on the chemical and physical properties of zinc oxide. The interfacial effect of zinc oxide/surfactants composites between zinc oxide and organic surfactants might be similar to the ZnO nanoparticles coated with sodium dodecylbenzenesulfonate reported by Wang.[18] X-ray photoelectron spectroscopic analysis indicates that the oxygen vacancies are formed in Zn-L nanocomposites. Many oxygen vacancies mainly located on the interface of the inorganic framework have interactions with interfacial capping surfactants, and surfactants might stabilize F-center-like oxygen vacancies. These interactions will lead to the formation of the trapped state that might form a series of metastable energy levels within the bandgap. Metastable energy levels are relatively long-lived and their optical transitions are dipole allowed. Thus, room temperature photoluminescence can be observed. Therefore, it could be inferred that the RTPL of the zinc oxide/surfactant mesophase might be induced by interfacial effects between the inorganic framework and the surfactants.

Conclusions

An ordered lamellar zinc oxide mesostructure was prepared in the presence of a neutral surfactant by self-assembly. Such Zn-L nanocomposites display new optical properties, such as a red-shift of absorption edge and room temperature photoluminescence. The absorption edge shifts to a low energy region (red-shift) because of the dielectric confinement effect. The interface effect between zinc oxide and surfactant is the main cause of the room temperature photoluminescence. These new optical properties of mesolamellar zinc oxide/surfactant nanocomposites also enhance their applications in optics.

Experimental Section

General: The structure was analyzed and characterized by X-ray diffraction (XRD, Rigaku D/max-RB diffractometer with Cu-K_α radiation, λ = 1.5418 Å). The sample was scanned from 1.2° to 20° (2θ) in steps of 0.02°. The scanning electron microscopy (SEM) photograph was obtained by JSM-6301F. Transmission electron micrographs (TEM) were made on a 200CX transmission electron microscope operated at 200 kV. Fourier transformed infrared (FTIR) spectra (4000–400 cm^{-1}) were recorded on a Perkin-Elmer Spectrum GX infrared spectrophotometer. Samples for FTIR were prepared using the KBr technology, which were calibrated by polystyrene. The composition of the Zn-L nanocomposite was determined by the X-ray photoemission spectra (XPS) recorded on a Perkin–Elmer PHI 5300 ESCA system with an Al-K_α X-ray beam and 250 W power. UV/Vis measurements were made with a UV2100 spectrophotometer. Photoluminescence (PL) measurements were carried out at room temperature using λ = 383 nm as the excitation wavelength with a HITACHI 850 type visible-ultraviolet spectrometer with a Xe laser as the excitation source.

Synthesis of ZnO/Dodecylamine Mesolamellar Nanocomposite: All chemical reagents used in the experiments were obtained from commercial sources as guaranteed-grade reagents and used without further purification or treatment. $ZnCl_2$ and DDA had purities of 98%. The composite was synthesized using a neutral dodecylamine ($C_{12}H_{27}N$, DDA) surfactant and zinc chloride ($ZnCl_2$). $ZnCl_2$ (1.36 g) was dissolved in distilled deionized water (DDW) (28 mL). DDA (0.74 g) dissolved in DDW (28 mL) was then added to the

$ZnCl_2$ solution under vigorous stirring. The synthesis mixture, possessing a molar ratio $ZnCl_2$:DDA:H_2O of 1.0:0.4:156, was stirred for 4 h before being aged at room temperature for 48 h. The solid product was then recovered by filtration and washed with water. Dry composite could be exposed to air without oxidation.

Acknowledgments

We thank Y. Fu for assistance with photoluminescence spectra measurements, X. Y. Ye for her help in the XPS, S.-Q. Sun for her help in the FTIR experiments, and Q. Cai for many helpful discussions. Funding from the Natural Science Foundation of Yunnan Province, China (2002Z0004Q) and the Project for Science and Technology of Yunnan University (2003Z003A) is gratefully acknowledged.

[1] S. H. Tolbert, P. Sieger, G. D. Stucky, S. M. J. Aubin, C. C. Wu, D. N. Hendrickson, *J. Am. Chem. Soc.* **1997**, *119*, 8652–8661.
[2] W. Y. Lin, W. Q. Peng, J. Z. Sun, J. C. Shen, *J. Mater. Chem.* **1999**, *9*, 641–642.
[3] Q. S. Huo, D. I. Margolese, U. Ciesla, D. G. Demuth, P. Y. Feng, T. E. Gier, P. Sieger, A. Firouzi, B. F. Chmelka, F. Chuth, G. D. Stucky, *Chem. Mater.* **1994**, *6*, 1176–1191.
[4] G. D. Stucky, Q. S. Huo, A. Firouzi, B. F. Chmelka, S. Schacht, I. G. Voigt-Martin, F. Schuth, *Stud. Surf. Sci. Catal.* **1996**, *105*, 3–28.
[5] A. Sayari, P. Liu, *Microporous Mater.* **1997**, *12*, 149–177.
[6] P. V. Braun, P. Osenar, S. I. Stupp, *Nature* **1996**, *380*, 325–328.
[7] Z. R. Tian, W. Tong, J. Y. Wang, N. G. Duan, V. V. Krishnan, S. L. Suib, *Science* **1997**, *276*, 926–930.
[8] K. G. Severin, T. M. Abdel-Fattah, T. J. Pinnavaia, *Chem. Commun.* **1998**, 1471–1472.
[9] Y. C. Kong, D. P. Yu, B. Zhang, W. Fang, S. Q. Feng, *Appl. Phys. Lett.* **2001**, *78*, 407–409.
[10] A.vav Dijken, E. A. Meulenkamp, D. Vanmaekelbergh, A. Meijerink, *J. Lumin.* **2000**, *87 – 89*, 454–456.
[11] Y. W. Wang, L. D. Zhang, G. Z. Wang, X. S. Peng, Z. Q. Chu, C. H. Liang, *J. Cryst. Growth* **2002**, *234*, 171–175.
[12] J. Zhang, L. D. Sun, C. S. Liao, C. H. Yan, *Chem. Commun.* **2002**, 262–263.
[13] Y. Q. Wang, S. G. Chen, X. H. Tang, O. Palchik, A. Zaban, *J. Mater. Chem.* **2001**, *11*, 521–526.
[14] S. Major, S. Kumar, M. Bhatnagar, K. L. Chopra, *Appl. Phys. Lett.* **1986**, *40*, 394–396.
[15] M. Chen, X. Wang, Y. H. Yu, Z. L. Pei, X. D. Bai, C. Sun, R. F. Huang, L. S. Wen, *Appl. Surf. Sci.* **2000**, *158*, 134–140.
[16] M. Koudelka, A. Monnier, J. Sanchez, *J. Mol. Catal.* **1984**, *25*, 295–2305.
[17] S. H. Yu, J. Yang, Y. T. Qian, M. Yoshimura, *Chem. Phys. Lett.* **2002**, *361*, 362–366.
[18] R. Y. Wang, X. C. Wu, P. F. Wu, B. S. Zou, L. Wang, J. Z. Xu, J. R. Xu, X. F. Wang, Z. J. Wang, J. X. Chen, *Acta Phys. Sin.* **1998**, *7*, 203–208.
[19] G. Mills, Z. G. Li, D. Mersel, *J. Phys. Chem.* **1988**, *92*, 822–828.
[20] X. C. Wu, B. S. Zou, J. R. Xu, B. L. Yu, G. Q. Tang, G. L. Zhang, W. J. Chen, *Nanostruct. Mater.* **1997**, *8*, 179–189.
[21] T. Takagahara, *Phys. Rev. B* **1993**, *47*, 4569–4585.
[22] B. L. Yu, C. S. Zhu, F. X. Gan, *Opt. Mater.* **1997**, *7*, 15–20.
[23] M. H. Huang, Y. Y. Wu, H. Feick, N. Tran, E. Weber, P. D. Yang, *Adv. Mater.* **2001**, *13*, 113–116.
[24] M. H. Huang, S. Mao, H. Feick, H. Yan, Y. Wu, H. Kind, E. Weber, R. Russo, P. D. Yang, *Science* **2001**, *292*, 1897–1899.
[25] J. J. Wu, S. C. Liu, *Adv. Mater.* **2002**, *14*, 215–218.
[26] K. Vanheusden, W. L. Warren, C. H. Seager, D. K. Tallant, J. A. Voigt, B. E. Gnade, *J. Appl. Phys.* **1996**, *79*, 7983–7990.

Received May 28, 2004

